

THIN, LIGHTWEIGHT, 18% EFFICIENT SPACE SILICON SOLAR CELL AND ARRAY

Yoon, S., Turner, G., Garboushian, V.
Amonix, Inc., 3425 Fujita Street, Torrance, CA 90505

ABSTRACT

The purpose of this paper is to report the progress achieved in the transition-to-production of the Radiation Hardened High Efficiency Silicon (RHES) solar cell first introduced in 1993 [1]. The RHES cell has a back-junction point-contact structure which has demonstrated higher than 18% AM0 efficiency. Two major improvements were accomplished: A) scaling up the cell from a laboratory prototype size to one suitable for space applications, B) optical matching of the cover glass to the light trapping structure of the cell surface.

In order to accommodate the larger cell size, it was necessary to completely re-design the junction and metalization patterns to increase production yields to acceptable and usable levels. To accomplish this, the junction area was increased with a corresponding decrease in metal periphery.

All solar cells for space applications must be glassed to protect the cell from damage from proton radiation, micrometeorites, and handling. The glassing process is critical to the RHES cell due to the fact that the bare cell surface depends, to some extent, on a light trapping textured structure to improve efficiency. Even with the best optically matched adhesives, some loss of output power was observed. After optimization of Anti-Reflective (AR) coatings, adhesive properties and application processes, more than 97% of the original power generating capability of the cell was retained.

INTRODUCTION

Amonix, Inc. reported the development of the Radiation Hardened High-Efficiency Space (RHES) solar cell in 1993 [1]. The RHES cell has a back-junction point-contact structure which has demonstrated higher than 18% AM0 efficiency. During the development of the RHES cell, small laboratory-size cells were utilized to minimize extraneous problems which would otherwise be encountered in working with large cell areas. These problems include series resistance, non-uniformity over a wafer for some critical parameters and yield. The end result was the successful development of the RHES cell baseline process and its subsequent optimization.

As the development effort transitioned from the demonstration stage to the production stage, the problems listed above needed to be addressed while maintaining the high level of performance achieved in the smaller laboratory size cells.

The incentive for production is based on the fact that the RHES cell has ideal structural features for utilization in space. The RHES cell is approximately 75~100 micron thin, with high efficiency for high power density per unit area and for high specific power (watts/kg). Also, the RHES cell has both electrodes on the backside of the cell allowing for the application of automated surface mounting technology for large area panels.

This surface mounting capability obviates the need for connectors for interconnecting the cells and offers a large flexibility for series and parallel connections to achieve optimal operating current and voltage levels for a panel.

In order to take advantage of the superior features of the RHES cell, it was decided to productize the RHES cell for space applications.

Productization

The productization of the RHES cell consisted of two steps: (1) scale-up of the small laboratory cell size to 2 cm X 2 cm and 2 cm X 4 cm sizes, (2) development and optimization of Anti-Reflective Coating (ARC) on the 2 cm X 2 cm cell to achieve the highest electrical conversion efficiency with a mounted cover glass.

The process of optimizing the external optical coating of the coverglass for selective transmission and reflection of ultraviolet and infrared light to realize the best overall performance from the coverglass, the coverglass adhesive, and the RHES cell was not carried out for this study due to the fact that the external coating over a coverglass can be completely de-couple from other optical components involved.

(1) Scale up of the RHES cell

The RHES cell is a back-junction cell [2,3]. The cell thickness is approximately 100 microns with a textured

front (sunward) surface with a multiple layer AR coating and pyramids of random size and distribution for achieving a high level of light trapping. The back-side of the RHHES cell contains a large number of individual P-type and N-type diffusions. Basically, the smaller size and closer proximity of the P and N diffusion junctions to each other can make the back-junction cell more efficient at the cost of manufacturing problems [2]. The high density of P and N junctions necessitate very narrow fingers in the first layer metal to channel the output of the small individual diodes to the cell terminals. Even though the second layer metal of a double layer metal is designed to minimize the total resistance, these long fingers have a finite resistance. As the cell size increases, the distance from the junction to termination and therefore the series resistance of the cell increases proportionally when the same design rule of the laboratory size cell is applied for scaling up.

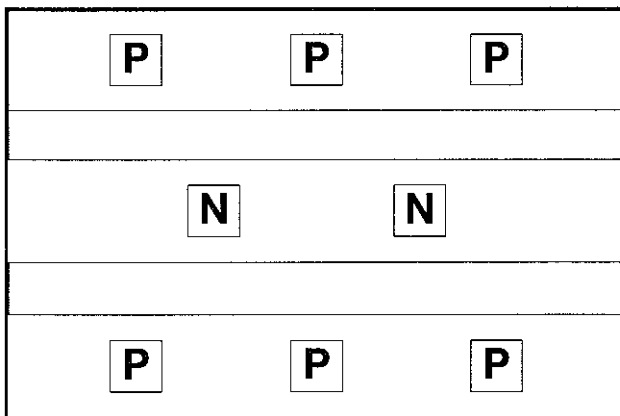


Figure 1: Schematic of RHHES

In Figure 1, the back-side point junction pattern and interdigitated metal finger pattern is schematically shown for the RHHES laboratory cell. The P and N diffusions are approximately 50 microns apart. Metal periphery density (length per unit cell area) for this pattern is approximately 9 meters/cm² of the cell active area affecting total resistance and cell yield adversely. The newly developed 2 cm X 2 cm RHHES cell's backside junction pattern uses rectangular patterns to maintain the adjacency of junctions as a point-contact design while reducing the total metal periphery. The RHHES 2 cm X 2 cm cells with the pattern have a metal periphery density of only approximately 2 meters/cm² and 30% more metal cross-sectional area for conduction. The design enabled high yield production with high performance by drastically lowering the probability for metal finger bridging while maintaining the desired proximity of P and N diffusions to each other using rectangular diffusion openings.

(2) Optimization of the AR coating for a glassed RHHES cell

The original RHHES laboratory cell has a randomly textured sunward top surface with an optimized ARC and

a reflective flat backside surface with silicon dioxide and aluminum metalization. This structure allows maximum light transmission from air to the optically dense silicon solar cell and maximum light trapping within the cell structure utilizing total internal reflections, producing a short circuit current density level higher than 50 mA/cm² under AM0 conditions.

The original RHHES cells were not glassed. However, any space applicable solar cell must be glassed to protect the cell from damage due to proton radiation and micrometeorite impingement in space environments and, also, due to handling during the assembly of cells onto a panel. Therefore, an optimization of ARC for coverglassed RHHES cells was carried out.

Since the primary goal for productization was utilization of the cell for low orbit applications, a ceria doped borosilicate coverglass at a thickness of 6 mils was selected. The refractive index of a coverglass with a nominal 5% cerium dioxide doping is typically 1.51 ± 0.02. The space qualified adhesives (encapsulants) have been typically transparent high-strength silicone rubber compounds. The refractive index for these compounds is typically 1.42 ± 0.02. Similar refractive index values for the two components reduces the second surface reflectance of the coverglass enhancing transmittance by approximately 4% compared to the value measured in air.

Because of the addition of the coverglass and adhesive, the original RHHES cell ARC structure, which was optimized for an air to ARC interface, had to be modified to accommodate the new adhesive to ARC interface. One can utilize ray tracing programs such as "TEXTURE" [4] to design near optimal ARCs by simulation, but it is important to verify the performance of such ARCs experimentally. In Figure 2, reflectance plots for bare flat silicon and randomly textured bare RHHES cells with air to silicon interface are compared at specific wavelengths of 200 nm to 700 nm in 100 nm increments.

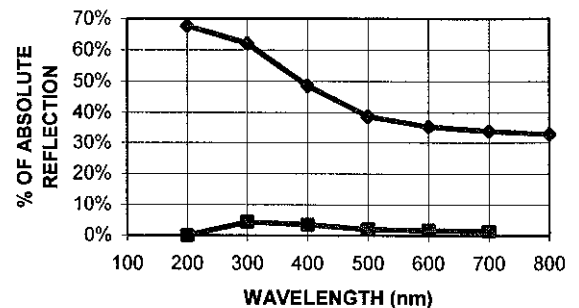


Figure 2: Reflectance Plots of Bare Flat (upper) and Textured (lower) Silicon

Notice the dramatic (order of magnitude) reduction of reflectance by a randomly textured silicon surface. In Figure 3, the reflectance of a single layer SiO₂ (n≈1.46) ARC with an air to SiO₂ interface is compared to the same reflectance curve of the randomly textured bare RHHES

cell shown in Figure 2. Notice the wavelength ranges affected by the addition of a SiO₂ single layer ARC. The reflectance around 400 nm and 700 nm are reduced.

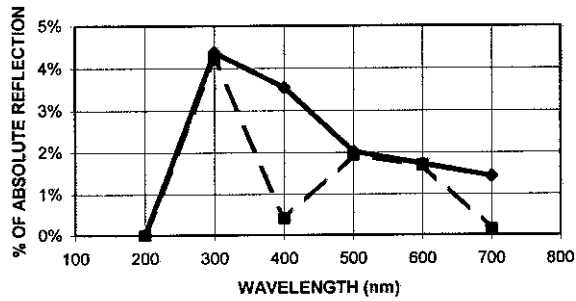


Figure 3: Reflectance Plots of RHES for Bare Textured (solid) and Single Layer SiO₂ ARC (dash)

In Figures 4-6, optical paths are compared for a single ray of 600 nm wavelength incident normal to the base of the texture pyramids for three cases. Figure 4 represents a situation, relative to Figure 2, of incident light entering silicon through the air/silicon interface. It shows the refracted light angle of 10 degrees into silicon which would experience a total internal reflection at the flat backside because, for the external medium of air, the critical angle will be 12.25°.

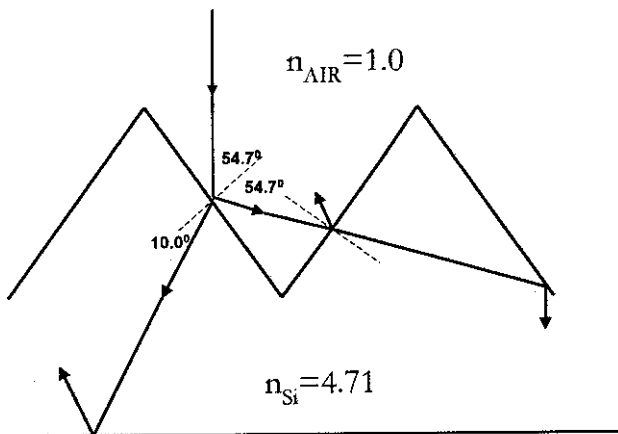


Figure 4: Optical Path for 600 nm Normal Incident Light to Bare Textured Silicon Surface from Air

Figure 5 describes a situation, relative to Figure 3, where incident light enters the silicon through the air/SiO₂/Si interface. It shows that only the direction of reflection changes while the refracted light enters the silicon at 10 degrees incident angle. The incident angle into silicon is the same as the Si/Si interface.

In Figure 6, a ray trace of a glassed single layer SiO₂ ARC is exemplified. Since refractive indices of adhesive and SiO₂ are so similar, the ray refraction is very minute at the adhesive/SiO₂ interface and enters silicon at a 14.2 degree incident angle.

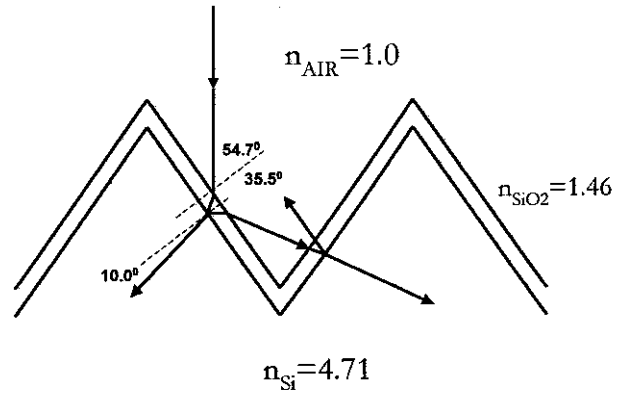


Figure 5: Optical Path for 600 nm Normal Incident Light Through Single Layer SiO₂ ARC Into Silicon

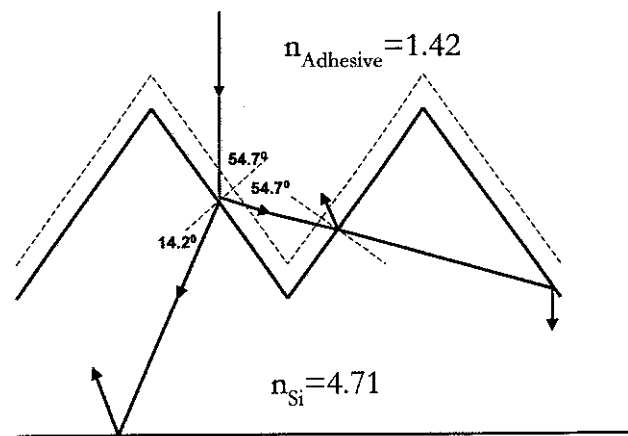


Figure 6: Optical Path for 600 nm Normal Incident Light Through Coverglass Adhesive Into Silicon

The incident angle into silicon only depends on the most external medium and is independent of ARC layers in the path. Due to the fact that the silicon has high refractive indices ranging from 3.53 to 6.80 at all wavelengths shorter than 1100 nm, the incident angle into silicon changes approximately one degree per refractive index change of 0.1 for the most external medium.

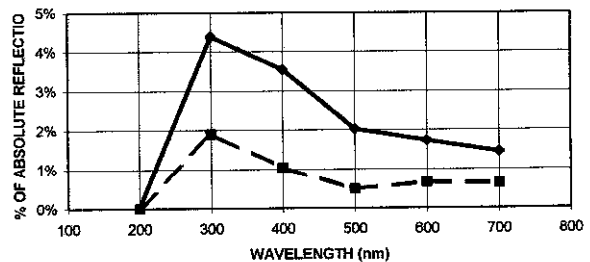


Figure 7: Reflectance Plots of RHES for Bare Textured and Optimized Tripple Layer ARC

In Figure 7, the reflectance of an optimized triple layer ARC consisting of $\text{SiO}_2/\text{SiOxNy}/\text{Si}_3\text{N}_4$ is shown along with the bare silicon random textured surface as measured in air.

(3) Experimental Measurements

In the course of developing the optimized ARC, a need for comparing two cells with different ARCs using the same cover glass and adhesive was encountered. If a coverglass was mounted on a cell using an adhesive, it is virtually impossible to disassemble and re-use the coverglass for other cells.

In order to accomplish the goal of re-using the same coverglass, the relationship, as discussed in the previous section, between the incident angle of the refracted light into silicon and the refractive index of the external medium for incoming light was utilized.

As a first approximation, de-ionized water was utilized to replicate the effects of the adhesive or encapsulant. Water, at 20°C has a refractive index of 1.333 for Sodium light with a wavelength of 589.3 nm which would generate a negligible optical path variation within the cell silicon since the incident angle into silicon will be less than one degree different compared to the "real" RTV-type adhesives. The incident angle into silicon would be approximately 13.3° instead of 14.2° for a 600 nm wavelength. Ethyl alcohol at 99.8% concentration could be utilized for the same purpose. Because its refractive index at 20°C is 1.360 for sodium light with a wavelength of 589.3 nm. If a more exact match to real adhesives is desired, an aqueous solution of sucrose can be utilized. A sucrose solution with 40~50% cane sugar concentration has a refractive index in the range of 1.40~14.2 at 20°C for sodium light [5].

RHHES cells (2 cm X 2 cm) retained over 93% and 97% of their original output power for uncoated coverglasses and MgF_2 AR coated coverglasses respectively.

ARRAY OF CELLS

The concept of a RHHES subarray or minimodule was introduced in the previous paper [1]. The introduction of a minimodule eliminated the need for connectors for interconnecting cells in-series or parallel strings. The developed minimodules which were fabricated on both rigid and flexible materials are reported as a separate paper in the 25th IEEE PV Conference [6].

This minimodule concept can be further extended directly onto a panel honeycomb and the panel can be subdivided into Power Generating Blocks (PGB). A large panel is sub-divided into many PGBs of nominal 50 watts of power having approximate dimensions of 50 cm X 50 cm. Each PGB contains 144 RHHES cells on a surface mount pattern area on a insulator directly laminated on a honeycomb structure. By utilizing 144 RHHES cells virtually any desired voltage and current can be obtained from each PGB.

CONCLUSION

A successful program to productize the RHHES cell from a small laboratory size to a practical size of 2 X 2 cm and 2 X 4 cm with coverglass and deployable in space environments is reported. A new rectangular junction design greatly enhanced the manufacturability of large size cells while maintaining the high performance of the "point contact" cell design. The ARC for the randomly textured RHHES cell has been optimized and the glassing process has been established. High efficiency silicon cells can be utilized in a variety of space missions in the future with proven reliability and performance as the comprehensive review of Iles described [7].

The productized and glassed RHHES cell and arrays have been tested for space qualification in most areas and reported [6].

ACKNOWLEDGEMENTS

The authors would like to thank the Naval Research Laboratory for their support of the development of the RHHES cell and the RHHES arrays. Dr. G. Vendura Jr. contributed significantly to the RHHES project through his advice and management of the space qualification portion of the project.

REFERENCES

- [1] Garboushian, V. and Yoon, S., "Radiation Hardened High Efficiency Silicon Space Solar", 23rd IEEE Photovoltaic Specialist Conference Proceedings, P1358 (1993)
- [2] Swanson, R.M., "Point-Contact Solar Cells: Modeling and Experiment", *Solar Cells*, 17, PP 85-118 (1986)
- [3] Yoon, S. and Garboushian, V., "Commercialization of High Concentration Back-Junction Point-Contact Photovoltaic Cells, Successful Pilot Production", 11th European Photovoltaic Solar Energy Conference, P 257 (1992)
- [4] Smith, A.W., Rohatgi, A. and Neel, S.C., "TEXTURE": A ray Tracing Program for the Photovoltaic Community", 21st IEEE Photovoltaic Specialist Conference Proceedings, P426 (1990)
- [5] Hodgman, C.D., Editor-in-Chief, "Handbook of Chemistry and Physics", 43rd Edition, *The Chemical Rubber Publishing Company*, P3013 (1961)
- [6] Garboushian, V., Turner, G., Yoon, S. and Vendura Jr., G.J., "Development of Back Junction Point Contact Photovoltaic Cells and Arrays for Space", 25th IEEE Photovoltaic Specialist Conference, Proceedings to be published (1996)
- [7] Iles, P.A., "Future Use of Silicon Solar Cells in Extraterrestrial Applications", *Progress in Photovoltaics: Research and Applications*, Vol 2, 95-106 (1994)